HAL open science

Conducting Polymers as Redox Electroactive Materials for Soft Microelectromechanical Systems

Kätlin Rohtlaid, Giao T.M. Nguyen, Caroline Soyer, Eric Cattan, Frederic Vidal, Cedric Plesse

To cite this version:

Kätlin Rohtlaid, Giao T.M. Nguyen, Caroline Soyer, Eric Cattan, Frederic Vidal, et al.. Conducting Polymers as Redox Electroactive Materials for Soft Microelectromechanical Systems. Nerea Casado; David Mecerreyes. Redox Polymers for Energy and Nanomedicine, Royal Society of Chemistry, pp.454-487, 2020, Polymer Chemistry Series, 9781788018715. 10.1039/9781788019743-00454 . hal-03539677

HAL Id: hal-03539677

https://hal.science/hal-03539677v1

Submitted on 6 Jul 2022

HAL is a multi-disciplinary open access archive for the deposit and dissemination of scientific research documents, whether they are published or not. The documents may come from teaching and research institutions in France or abroad, or from public or private research centers.

L'archive ouverte pluridisciplinaire **HAL**, est destinée au dépôt et à la diffusion de documents scientifiques de niveau recherche, publiés ou non, émanant des établissements d'enseignement et de recherche français ou étrangers, des laboratoires publics ou privés.

Distributed under a Creative Commons Attribution - NonCommercial 4.0 International License

Conducting Polymers as Redox Electroactive Materials for Soft Microelectromechanical Systems

K. ROHTLAID,[a] T. M. G. NGUYEN,[a] C. SOYER,[b] E. CATTAN,[b] F. VIDAL[a] AND C. PLESSE*[a]

[a] LPPI (EA2528), Institut des Matériaux, Université de Cergy-Pontoise, 5 mail Gay Lussac, Neuville sur Oise, F-95031 Cergy Cedex, France;
[b] Univ. Polytechnique des Hauts de France, CNRS, Univ. Lille, Yncrea, Centrale Lille, UMR 8520 - IEMN, DOAE, F-59313 Valenciennes, France
*Email: cedric.plesse@u-cergy.fr

12.1 Introduction

Artificial muscle is a general term for a group of materials or devices that are intended to mimic the functionality of natural muscles. Electroactive polymers (EAPs) have been intensively investigated for this purpose, since they are soft, lightweight, easily processed and manufactured. The main functionality of these materials is that through external electric stimulus they are able to generate reversible contraction and expansion, which leads to changing their shape or size similarly to natural muscles. Based on their activation mechanism, EAPs are classified into two main categories: electronic EAPs and ionic EAPs.

The electronic EAPs are driven by an electric field[1,2] and this group includes dielectric elastomers, ferroelectric polymers, also called piezoelectric polymers, and electrostrictive polymers.[3–6] In an example of dielectric elastomer actuators, the actuation mechanism is caused by the electrostatic

forces between two electrodes, which apply Maxwell pressure to a soft dielectric elastomer and result in plane expansion of the device. Electronic EAPs are known to produce relatively large actuation forces, respond rapidly (order of a millisecond) and to operate in open air for a long time. A perceived drawback with these types of actuators is their need for high voltage (up to 150 MV m^{-1}), although some recent research has succeeded in reducing it significantly,[7] which may be disadvantageous for many applications. Indeed, high voltage could be close to the electrical breakdown level and even dangerous if not handled carefully.

The ionic EAPs are driven by the electrical potential which induces mobility or diffusion of ions between their two electrodes. This group of materials includes electronically conducting polymers (ECPs), ionic polymer–metal composites (IPMC), carbon nanotubes (CNTs), carbide-derived carbon (CDC) and ionic polymer gels (IPGs).[2,8–18] Compared to the electronic EAPs, the main advantage of the ionic EAPs is their low operating voltages (1–5 V). Additionally, they are also capable of generating an electrical signal in response to mechanical stimulation, *i.e.*, they behave as sensors, providing dual behaviour, *i.e.*, actuation/sensing, as the so-called proprioception of biological muscles.

Among ionic EAPs, most of the investigated materials are based on a capacitive behaviour where ions are attracted by oppositely charged electrodes. However, the working principle of ECP-based EAPs is significantly different due to the redox nature of the polymer. Indeed, ECP actuators are driven by the ion diffusion inside/outside the polymer during a redox process in the presence of an electrolyte, resulting in volume variation of the materials. ECPs are flexible and lightweight materials, able to operate at low potentials and offer the possibility of processability and miniaturization, making them attractive for the development of soft microelectromechanical systems (MEMS).

MEMS is a generic term to describe multifunctional and intelligent integrated microscale systems combining different elements (electrical, mechanical, optical, magnetic, thermal, chemical, fluidic). They are usually fabricated with semiconductor processing techniques. Miniaturization and MEMS fabrication allow reducing the size and manufacturing costs and could possibly improve the performances of the microdevices. MEMS are usually classified into two main categories: actuators and sensors. Actuators are devices able to produce mechanical work from energy (electrical, chemical, mechanical, thermal, magnetic, *etc.*) and sensors are devices able to convert a specific variable (pressure, strain, flow, heat, chemicals, biological elements, *etc.*) into a measurable signal. Microfabrication technology has advanced over the years and allowed the development of different MEMS, used in a wide range of applications (aeronautics, satellites, automotive, computers, video game consoles, displays, printers, phones, medical devices, *etc.*) covered by most scientific and technical fields (physics, chemistry, materials science, biology, medicine, electronics, mechanics, computer science, robotics, *etc.*). Nevertheless, the general and powerful trend of moving from stiff to soft electronics requires the synthesis, understanding and integration of new smart polymeric materials.

This chapter focuses on ECPs as redox polymers for the development of soft actuators and more specifically on their potential for being used as soft MEMS in soft electronics (flexible substrates, soft robotics, biomedicine, microbiology, *etc.*).

After a brief description of the basics on ECPs (discovery history, structures and conductivity mechanism), the chapter focuses on their synthesis and on their use as active layers for ionic actuators. The different strategies for the development of ECP-based microactuators, the possibility to integrate them into complex microsystems, and the issues and challenges that these exciting materials are still facing are then presented and discussed.

12.2 Electronically Conducting Polymers

Conducting polymers were discovered in 1977 after a mistake by a PhD student in Shirakawa's group, who applied a thousand times higher amount of Ziegler-Natta catalyst into acetylene. The accelerated reaction rate resulted in the formation of a silvery film on the walls of the reaction vessel.[19] This obtained metallic-looking material was then additionally investigated by MacDiarmid and Shirakawa. It was discovered that the material is conductive because of the conjugated double bonds and the obtained iodine-doped polyacetylene resulted in an electronic conductivity of 10^3 S cm^{-1}. Shortly after this discovery, a series of conducting polymers, like polypyrrole (PPy), polyaniline (PAn) and polythiophene (PTh) were reported and promoted the research of conducting polymers. In 2000, Heeger, MacDiarmid and Shirakawa shared the Nobel prize "for the discovery and development of conducting polymers" (polyacetylene).[20]

The electronically conducting polymers (ECPs) or π-conjugated polymers have a bonding pattern consisting of alternating single (σ-bonds) and double (π-bonds) carbon bonds along the backbone of the polymer chain. Such conjugation leads to a structure with continuous overlapping π-molecular orbitals along the polymer backbone. In their neutral form, ECPs are insulators or poorly conducting semiconductors since they do not have intrinsic charge carriers.

The conductivity is obtained by partial addition (n-doping) or removal (p-doping) of electrons to or from the neutral and insulating polymer chains, which provides charge carriers able to move along the orbital system. Depending on their doping level, the conductivity values of ECPs can range between insulators and conductors.[21] Doping is generally a reversible oxidation-reduction reaction by chemical or electrochemical means and results in positive or negative charges on the polymer chain. Most commonly, p-doping is used because it is more stable compared to n-doping and will be the focus of the subsequent discussion. During p-doping, π-electrons are removed from the polymer chains. As a consequence, surrounding anions, acting as dopants, are incorporated within the polymer chains to maintain the charge neutrality of the

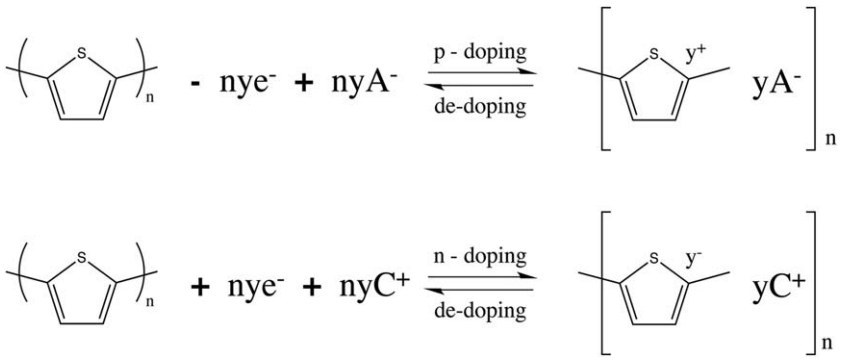

Figure 12.1 Reversible p- and n-doping mechanisms of polythiophene.

system. The de-doping reaction corresponds to a return to the neutral state of ECPs (see Figure 12.1).

Several types of charge carriers may appear during p-doping and for ECPs they are typically referred to as polarons, bipolarons or charged solitons.[22,23] According to the band theory, the electrical properties of these materials are determined by their electronic structure and the electrons move within discrete energy states, called bands. The highest occupied molecular orbital (HOMO) corresponds to the valence band (VB), usually described for inorganic semiconductors and the lowest unoccupied molecular orbital (LUMO) to the conduction band (CB). The energy difference between them is called the band gap (see Figure 12.2). The bands should be partially filled, in order to obtain the electrical conductivity of the materials. Semiconductors have completely full VB and completely empty CB and need to be doped to change their band structures and to become conductors. In the example of p-doped ECPs, the polarons are created when one electron is removed from the top of the VB. The removal of the second electron on a chain results in the formation of a bipolaron through dimerization of two polarons. The number of polarons and bipolarons increases with the doping level. High doping levels lead to new energy bands through which electrons can flow and metal-type conductivity can be achieved.[24]

Therefore, the appearance of the charge carriers along the macromolecular chains results in drastic changes in the electrical properties of the polymers. Depending on the state of the polymer (neutral or doped) and the type of doping, the electronic properties of ECPs can be very different. Some conjugated polymers with their chemical structures, doping nature and conductivities are presented in Table 12.1.

The reversible redox process, *i.e.*, the ability to switch between the two states (neutral and oxidized/reduced) is then a property of conducting polymers. In addition to changing the conductivity, several other properties are dependent on the redox level, which allows their use in different applications such as supercapacitors, electrochromic devices and actuators. This work and the next sections will be focused on actuator-related applications.

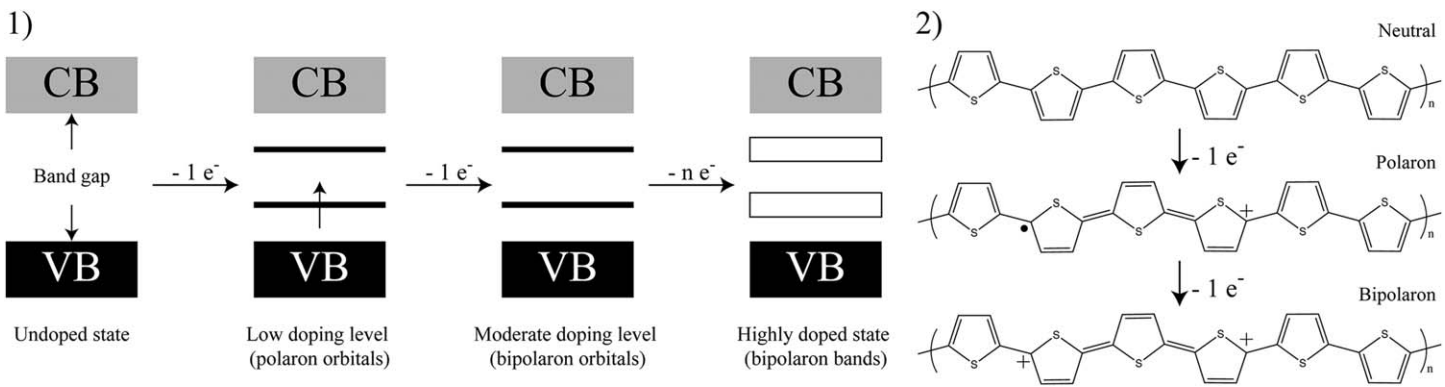

Figure 12.2 Schematic representation of a: (1) band structure as a function of doping level; (2) p-doping of polythiophene.

Table 12.1 Doping nature (n or p), conductivities and structures for some electronically conducting polymers.

Polymer	Doping nature	Conductivity ($S\,cm^{-1}$)	Structure
Polyacetylene (PA)	n, p	10^5 [25]	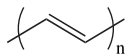
Polyaniline (PANI)	n, p	10^2 [26]	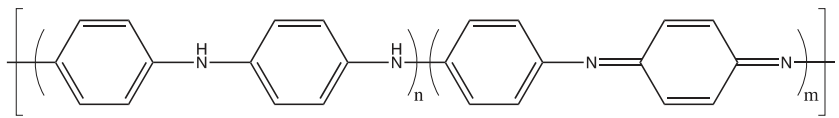
Polypyrrole (PPy)	p	10^3 [27]	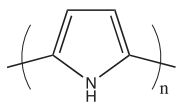
Polythiophene (PT)	p	10^3 [28]	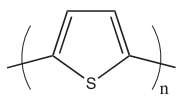
Poly(3,4-ethylene-dioxythiophene) (PEDOT)	n, p	10^3 [29]	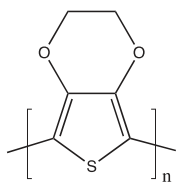

12.3 Electronically Conducting Polymer Actuators

Electronically conducting polymer actuators are electromechanically active devices that are able to change their shape or size in response to the electrical stimulus. They have attracted lots of interest due to their low operating voltages, relatively large forces and biocompatibility.[11] The following subsections will describe first the working principle of ECPs and different synthesis methods used in the actuators field. Moreover, an overview of the ECP actuators will be given based on their operation environment (in solution and in open air).

12.3.1 Oxidation, Reduction and the Volume Variation of Conducting Polymers

The working principle of ECP actuators is based on the electrochemically driven insertion or expulsion of ions, occurring during their reversible redox process. During the oxidation-reduction process, positive charges are created (p-doping) or removed (de-doping) from the polymer backbone. As a consequence of this charge modification, ions from a surrounding electrolyte are being inserted in or expelled from the polymer chains in order to maintain the charge neutrality. Consequently, this ion exchange mechanism induces the expansion or contraction of the polymer, leading to a volume variation of the ECPs.[30–32]

The switching between oxidized and reduced state can be achieved either by (1) expulsion of anions or (2) insertion of cations:

(1) During oxidation of the conducting polymer, the (electro)chemically generated positive charges will be compensated by the insertion of anions (and accompanying solvent molecules) within the material, leading to a volume expansion. During reduction (de-doping), positive charges are removed and anions are expelled, leading to a volume contraction.[33,34]
(2) If the polymer is doped during the synthesis with large and immobile anions, or if the mobility of anions is low compared to that of cations, the opposite mechanism takes place. During oxidation, cations will be expelled from the material in order to maintain the electroneutrality, resulting in volume contraction. During reduction, cations are inserted among the polymer chains and a volume expansion can be observed.[35,36]

Figure 12.3 illustrates these two reversible mechanisms during redox reaction with poly(3,4-ethylenedioxythiophene) (PEDOT) chosen as an example.

In some cases, when both ions have comparable size and/or mobility, the two redox mechanisms can take place concomitantly or consecutively. This results in opposite volume variations and can lead to a decrease in final

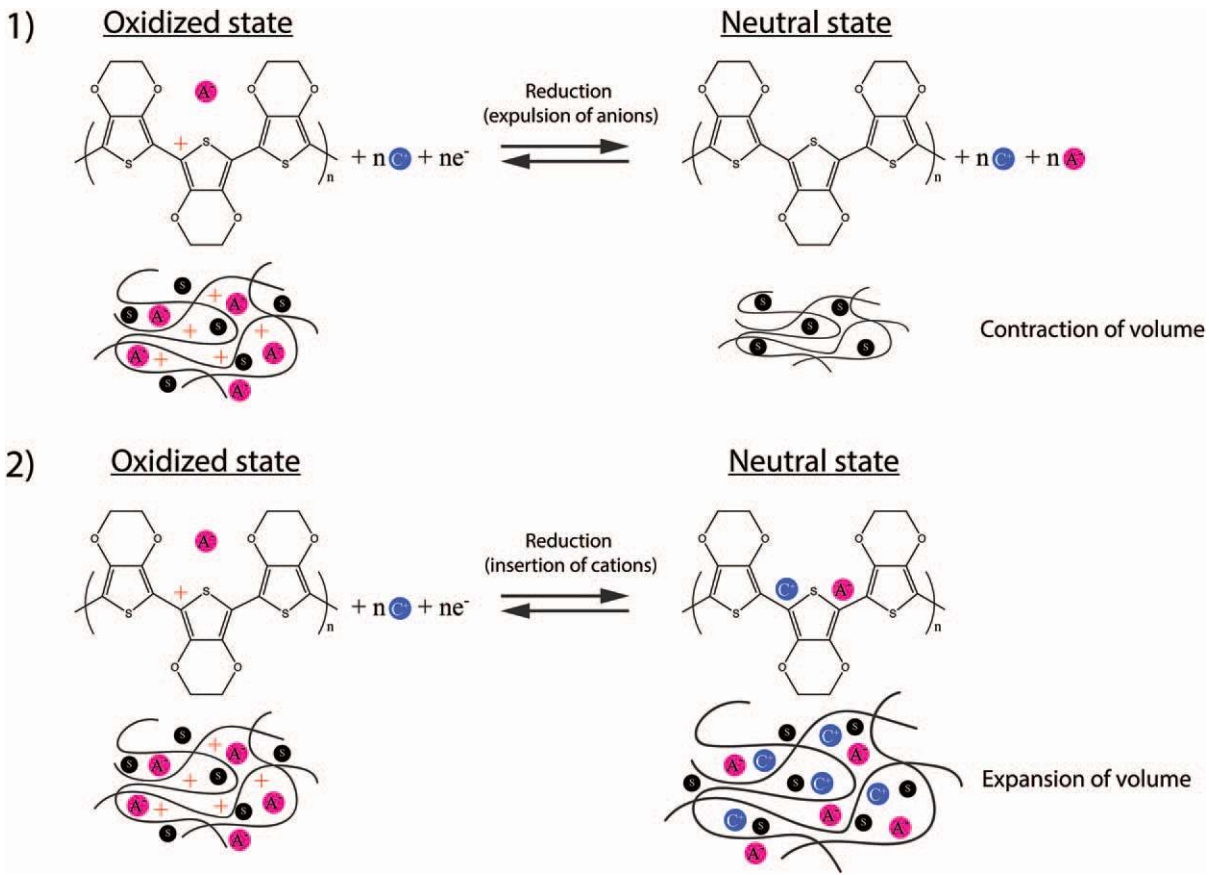

Figure 12.3 Volume variation mechanism of conducting polymers on an example of PEDOT.

expansion/contraction.[37] In addition to the size and mobility of ions, also the nature of the solvent and conformational changes in the polymer can affect the redox process and consequently also the volume changes.[38–40] In general, the ion exchange mechanism is the main factor concerning the redox process and volume variation of ECPs. This unique volume-changing characteristic of ECPs can be used for actuator applications.

The volume variation of electronically conducting polymers, *i.e.*, the strain ε, depends on the volumetric charge density ρ ($\mathrm{C\,m^{-3}}$) of the ECP and on an empirical electromechanical coupling coefficient, so-called strain-to-charge ratio α ($\mathrm{m^3\,C^{-1}}$), by the relationship: $\varepsilon = \alpha\rho$.[41] Therefore, high volume variation requires high electrochemical charge density, *i.e.*, a high number of expelled/inserted ions, and high elementary volume variation for each exchanged charge. The sign of α depends on the involved mechanism. A positive value of α corresponds to an anion mechanism, since during oxidation ($\rho > 0$), the insertion of the negatively charged ions in the ECP promotes an expansion and therefore a positive volume variation ($\varepsilon > 0$). On the opposite side, a negative value of α corresponds to a cation mechanism since during oxidation ($\rho > 0$), the expulsion of the positively charged ions from the ECP promotes a contraction, resulting in a negative volume variation ($\varepsilon < 0$).

12.3.2 Synthesis of Conducting Polymers for Actuator Purposes

There are several possibilities to synthesize conducting polymers, but the most commonly used and described methods in the literature for ECP actuators are the chemical and electrochemical oxidative polymerizations. Both of these methods lead to p-doped conducting polymers, *i.e.*, in their oxidized state after synthesis. The choice of the method (chemical or electrochemical) has an effect on the resulting polymer's morphology, crystallinity, doping level, conductivity and molecular weight. The most commonly used and described ECPs for actuator applications are PANI, PPy and PEDOT.

The electrochemical synthesis of ECPs is usually carried out employing the galvanostatic or potentiostatic method or by cyclic voltammetry. This synthesis method allows the control of a wide range of parameters, such as the nature of counter-ions, usually chosen according to the solubility in the selected solvent, the polymerization temperature and the potential or current.[42] It is an effective process which allows reproducibility and more precise control on electropolymerization kinetics, morphology and the thickness of the resulting ECP layers. However, the process is limited to the synthesis of electronic conducting substrates and large deposition areas can suffer from the lack of film uniformity. Usually thin metal layers are used in order to deposit the ECP layers. Recently, Temmer *et al.* proposed a different method for ECP actuators by replacing the metal layer with chemically oxidized PEDOT, where afterwards PPy was electrochemically deposited.[37,43]

The chemical oxidative polymerization method is realized in the presence of a monomer (pyrrole, EDOT, *etc.*) and an oxidant. The most commonly

used oxidants for chemical oxidation are iron(III) chloride ($FeCl_3$) and iron(III) tosylate [$Fe(OTs)_3$]. Using $FeCl_3$ as the oxidant for the chemical oxidation, directly mixed with the monomer, results in highly conductive, but brittle and insoluble powder, which is usually not applicable for self-standing film or actuator fabrication.[42] Host materials are most commonly used for ECP actuators in order to obtain the ECP as a film. In this case, the host material is swollen with the monomer, which is then immersed into the oxidant solution and allows the formation of ECP film directly at the interface of the host material.[44] Generally, the chemical oxidation is a cheap and facile method and the polymerization can be obtained on nonconductive substrates, which is not possible with electrochemical polymerization.

Vapour phase polymerization (VPP) is another route of chemical oxidation, which is usually carried out by introducing the monomer vapour to the oxidant-covered substrate. This polymerization method was first described by Mohammadi *et al.* in 1986 and allows the formation of thin and uniform ECP layers.[45]

ECPs are also commercially available, for example in the form of poly(3,4-ethylenedioxythiophene):poly(styrene sulphonate) (PEDOT:PSS) dispersion. This ink-type conducting polymer dispersion was first commercialized under the trade name of Baytron® and is currently manufactured by Heraeus under the trade name of Clevios™.[46] It is the most successful commercialized conducting polymer ink in terms of practical applications (conductive coatings, antistatic coatings, electroluminescent devices, capacitors, *etc.*). A deep blue PEDOT:PSS microdispersion can be obtained through aqueous oxidative polymerization of the hydrophobic EDOT monomer in the presence of polystyrene sulphonic acid (PSS) (see Figure 12.4a). The resulting aqueous mixture is a colloidal dispersion of PEDOT:PSS particles with hydrophobic and positively charged (doped) PEDOT core surrounded by hydrophilic and negatively charged PSS shell (see Figure 12.4b).[47] The PSS has two functions in the PEDOT:PSS complex: (i) it serves as the charge-balancing counter-ion for the doped PEDOT, and (ii) it disperses and stabilizes the PEDOT particles in water and other solvents.[42,48] The ink-type nature of PEDOT:PSS dispersion has the advantage of easy processing through various methods, such as drop casting, spray coating, spin coating and ink-printing techniques.[49–58] The resulting material possesses many unique properties, such as flexibility, intrinsic conductivity, biocompatibility and high chemical stability.[42] The electrical conductivity of PEDOT:PSS is influenced by different synthetic conditions, processing additives or post-treatment techniques.[59–66]

12.3.3 Conducting Polymer Actuators Operating in Liquid Electrolyte

The use of conducting polymers as actuators was first demonstrated by Baughman in the 1990s (see Figure 12.5b).[8,11,68] This actuator was constructed to operate in electrolytic solution in a bending mode. Ever since, great advances and improvements in this field have been made and

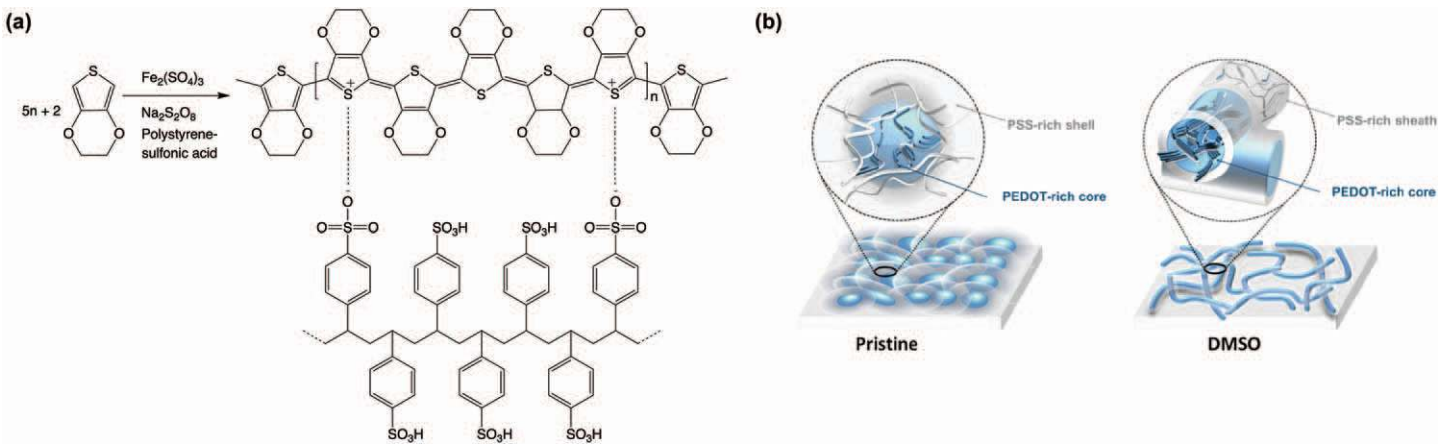

Figure 12.4 (a) Oxidative polymerization of EDOT monomer in the presence of PSS and a primary structure of PEDOT:PSS; (b) scheme representing the morphology and effects of additives of PEDOT:PSS.
Reproduced from ref. 67 with permission from the American Chemical Society, Copyright 2019.

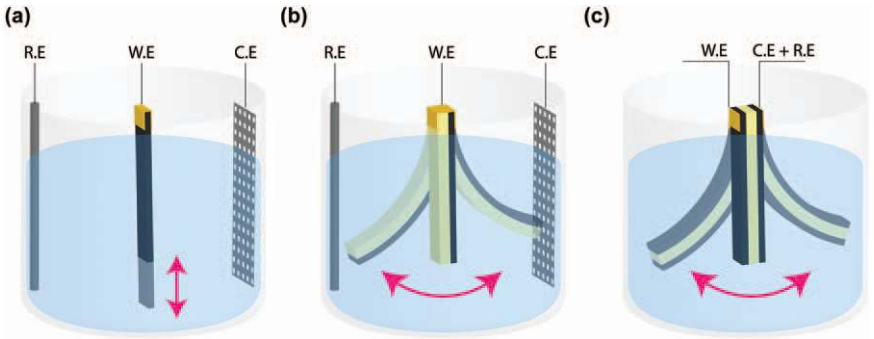

Figure 12.5 Schematic view of different actuators operating in liquid electrolyte in a three-electrode configuration: (a) freestanding linear actuator, (b) bilayer bending actuator and (c) trilayer bending actuator.

reported. Conducting polymer actuators can be divided into different categories based on: active ECP material, operating environment (in solution, open air), number of layers (freestanding, bilayers, trilayers), motion type (linear or bending) and dimensions (nano-, micro-, macroscale). The overview of ECP actuators in these sections is based on their operating environment and will be discussed subsequently.

Conducting polymer actuators operating in liquid electrolyte can be constructed as freestanding films, bilayer actuators or trilayer actuators. The freestanding films (see Figure 12.5a) were initially used in their most basic form to understand the fundamental performances of conducting polymers. The volume change of the ECP is isotropic, but if the configuration of the polymer is anisotropic as a film, a linear deformation can be obtained.[69,70]

Bilayer actuators are usually two-layer structures consisting of a passive layer (constant volume) and an ECP layer (see Figure 12.5b). The fabrication of a bilayer actuator is usually obtained by the electrochemical synthesis of a conducting polymer layer directly on a flexible substrate with a thin layer of sputtered metal.[12,71–73] The substrate, *i.e.*, the passive materials, can be a plastic or a piece of paper.[11,74–77] Another possibility to realize bilayer actuators is to fabricate both layers (passive and conductive) separately and later manually attaching them.[78,79]

The actuation of these freestanding and bilayer devices has to be performed in a three-electrode configuration when immersed in liquid electrolyte. The ECP layer acts as a working electrode (WE). Metal grids or wires (platinum, gold, silver, stainless steel) are usually used as a counter electrode (CE) and classical reference electrode (RE) is added to control the potential of the system. The electrochemical oxidation/reduction of the WE when applying potential difference or current results in reversible volume variation of the ECP layer and consequently leads to a linear (freestanding film) or bending (bilayer actuator) movement.[35,70,80–83]

Two-electrode configuration can be used if the device is elaborated with a trilayer configuration. In this case, a second ECP electrode is deposited on

the other side of the passive film (see Figure 12.5c). One ECP layer is then connected to the WE and the second ECP layer to the CE + RE. Electrical stimulation of the trilayer, still immersed in electrolyte, promotes opposite electrochemical reactions in the electrodes, one being oxidized (anode) while the second one (cathode) is concomitantly reduced. As a consequence, one layer expands while the other contracts, leading to the bending movement of the actuator.[84,85] A trilayer configuration has the advantage of producing higher output forces compared to the bilayer actuator due to the presence of the two electrodes instead of one. However, the operation in liquid electrolyte may reduce their potential areas of applications.[79,86]

12.3.4 Conducting Polymer Actuators Operating in Open Air

Air operation of ECP actuators allows broadening of their application field. Since these ionic actuators require an ion source in order to operate, the strategy was to replace the previously described passive film for trilayer configuration with an ionically conducting film, behaving as an ion reservoir. In other words, the necessary ions are incorporated directly in the self-standing trilayer device (see Figure 12.6).

The redox process takes place in the same way as for the trilayers in the liquid electrolyte, except that the ion exchange occurs between the electrodes with the electrolyte are directly included in the separator membrane. When applying a potential, the ions will be inserted into one ECP layer and expulsed from the other ECP layer resulting in an open-air bending movement of the actuator. The ion reservoir membranes and the open-air trilayer actuators will be described in the following sections.

12.3.4.1 Ionic Membranes for Conducting Polymer Actuators

Different ECPs (PPy, PEDOT, *etc.*) and different ion reservoir membranes (gel electrolyte, porous membrane filled with electrolyte, solid polymer electrolyte) have been used for actuator fabrication.[80,87–91] The ion reservoir membrane has an important role in the actuator configuration by providing the system with ionic conductivity and mechanical properties. Nowadays,

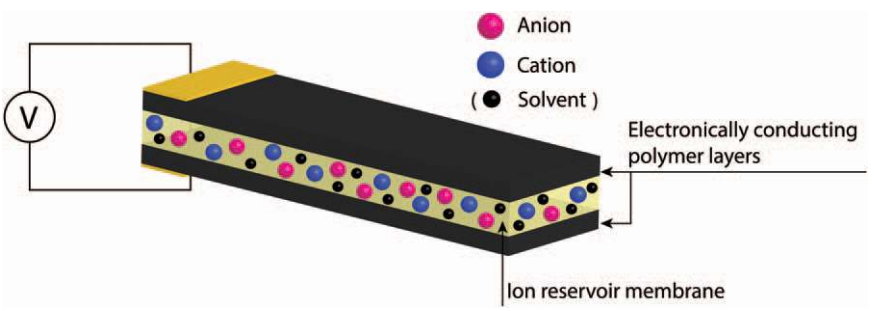

Figure 12.6 Schematic view of a trilayer actuator for operating in the open air.

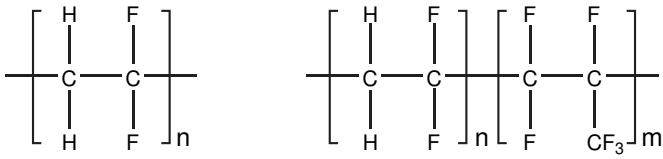

Scheme 12.1 Chemical structures of poly(vinylidene fluoride) (PVdF) and poly(vinylidene fluoride)-*co*-hexafluoropropylene (PVdF-HFP).

most commonly used ion reservoir membranes for actuators are based on microporous poly(vinylidene fluoride) (PVdF)-containing electrolyte, based on single networks or on an interpenetrating polymer network (IPN) architecture swollen with electrolyte.

Poly(vinylidene fluoride) (PVdF) and its copolymers (Scheme 12.1) are widely used as porous membranes mainly for filtration purposes.[92,93] For actuation applications, they are mostly used because of their commercial availability, allowing fast and simple actuator fabrication and because of their porous nature allowing strong anchoring of the ECP layer to avoid delamination issues. PVdF is a semicrystalline polymer with the repeat unit of $-(CH_2CF_2)_n-$, presenting high mechanical strength and stability, good chemical resistance and it is often used as a commercial thermoplastic membrane (Millipore®).[94] This polymer presents good compatibility with liquid electrolytes, which simply fill the porous structure without solvating the membrane. The porous copolymer poly(vinylidene fluoride)-*co*-hexafluoropropylene (PVdF-HFP) is often used for electrochemical applications due to good electrochemical stability.[95,96] PVdF-HFP has both, crystalline VdF and amorphous HFP units. The crystalline phase provides the structural properties to support a freestanding film and the amorphous phase is capable of trapping a large amount of electrolyte which contributes to increasing the swelling rate of the polymer and then provides the ionic conductivity.

The use of single networks for ion reservoir membranes has been demonstrated by different research groups. The first ion reservoir membrane for open-air actuators was developed by Sansiñena *et al.* and was based on poly(epichlorohydrin-*co*-ethylene oxide) [P(ECH-*co*-EO)] and lithium perchlorate ($LiClO_4$).[87] The resulting gel-like membrane presented good ionic conductivity but relatively poor mechanical properties. Vidal *et al.* demonstrated the fabrication of a dangled chain PEO network since it favours ionic mobility.[44] The single PEO network was obtained by free-radical copolymerization of poly(ethylene glycol) dimethacrylate (PEGDM) and poly(ethylene glycol) methyl ether methacrylate (PEGM), later swollen in 0.1 M $LiClO_4$ aqueous solution. However, the resulting material presented poor mechanical properties due to the brittle nature of this PEO network and was not satisfying as an ionic reservoir membrane for actuator fabrication. Cho *et al.* proposed the use of a high-molecular-weight nitrile butadiene rubber (NBR) network swollen in ionic liquid as an ionic membrane for actuator fabrication.[97,98] The presence of NBR could fulfil the mechanical requirements,

but the membrane's ionic conductivity was not sufficient for use as an ionic reservoir. The use of polyurethane (PU) containing $Mg(ClO_4)_2$ as an ion reservoir membrane was demonstrated by Choi *et al.*,[99] however with poor ionic conductivity. The ionic conductivity of the similar PU system was further improved by the group of Okuzaki using ionic liquid (IL) as an electrolyte to develop IL/PU gels suitable for the actuator fabrication.[100,101]

Another type of ionic membrane for actuators is based on interpenetrating polymer network (IPN) architecture containing an electrolyte. IPNs are defined as the combination of two or more cross-linked polymers, synthesized in the presence of each other.[102,103] It is the only way to combine cross-linked polymer networks and provide usually good dimensional and morphological stability. Depending on their synthesis pathway, the relative weight ratio of components and their relative cross-linking kinetics, different morphologies can be obtained. In order to combine the intrinsic properties of each polymer partner, co-continuous morphology across the material is usually desired. Semi-IPNs can also be obtained if one of the polymer partners is not cross-linked. In this case, it remains as linear macromolecules interpenetrated and entangled in the cross-linked structure of the second network.

There are many ways to synthesize IPNs. In the *sequential pathway*, the precursors of the second network (monomer 2, cross-linker, initiator) are introduced, usually by swelling, and subsequently polymerized in an already-formed single network of the first partner. In the *in situ* pathway, all the precursors, *i.e.*, monomers, cross-linkers, initiators and/or catalysts, are mixed together, eventually with a solvent, and polymerized. Polymerization of both networks can be performed simultaneously or sequentially. When networks are polymerized simultaneously, it corresponds to the *in situ simultaneous pathway.* It must be mentioned here that noninterfering polymerization mechanisms are used, like free-radical polymerization for one network and step polymerization for the other. If networks are polymerized sequentially, it corresponds to the *in situ sequential pathway*. In this case, the polymerization mechanism can be similar but monomers have to present significantly different reactivity (see Figure 12.7).

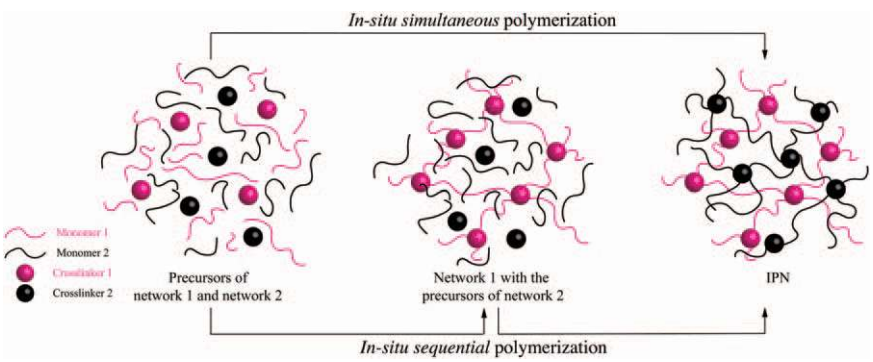

Figure 12.7 Schematic view of the two polymerization routes to fabricate IPNs from the precursors of network 1 and network 2.

The first IPN-based membrane for ionic reservoir in actuator application was elaborated as poly(ethylene oxide) (PEO)/polycarbonate (PC) IPN, obtained by *in situ sequential* polymerization. From a reactive mixture containing all the network precursors, the PEO network was obtained by free-radical copolymerization of poly(ethylene glycol) dimethacrylate (PEGDM), poly(ethylene glycol) methyl ether methacrylate (PEGM) and PC network by free radical polymerization at higher temperature of the less reactive monomer di(ethylene glycol) bis(allyl carbonate) (DEGBAC).[91] Unfortunately, this membrane was not suitable for long-life operation of the actuator due to the brittle nature of PEO and PC and finally the poor mechanical properties of the resulting IPNs after swelling with electrolyte. Optimized materials were proposed later by replacing the glassy PC network with those based on elastomers, such as polybutadiene (PB),[104,105] polytetrahydrofurane (PTHF)[106] and NBR.[107] When phase co-continuity is obtained, the PEO phase can act as an efficient ionic conducting medium while the elastomer phase acts as mechanical reinforcement due to its rubber properties. Upon swelling in an electrolyte, the resulting membrane can be used as an ionic reservoir for actuators. Ionic conductivities up to 10^{-3} S cm^{-1} and strain at break above 150% have been demonstrated using 1-ethyl-3-methylimidazolium bis(trifluoromethylsulphonyl)imide (EMImTFSI) as electrolyte.[108] These results demonstrated the advantage of IPN architecture in the synthesis of highly ionically conductive and robust ion reservoir membranes by combining the intrinsic properties of each partner. The chemical structures of these used polymers are illustrated in Scheme 12.2.

12.3.4.2 Trilayer Conducting Polymer-based Bending Actuators

The first trilayer actuator operating in open air was described by the MacDiarmid group in 1994.[109] This electrochemical actuator consisted of two PANI films which were affixed on both sides of double-sided cellophane tape and wetted in hydrochloric acid aqueous solution. The deformation of the actuator at maximum bending was estimated to be approximately 1%, with an applied voltage of 4.0 V. A few years later, the wetted cellophane tape was replaced by a gel-like membrane.[87] The polymeric electrolyte solution was dropped on two electropolymerized PPy electrodes, which were affixed together after solvent evaporation. The actuator resulted in 90° angular bending and demonstrated efficient fabrication of all polymer actuator.

The development of actuators had to overcome different problems related to the mechanical properties or lifetime of the actuators. The gel electrolytes that were used as ion reservoir membranes for actuators were mostly insufficient due to poor mechanical properties. Another common problem was the use of electrolytic solutions (salt/organic solvent or salt/water) which were limiting the lifetime of the actuators due to the solvent evaporation. This issue can be solved if an ionic liquid is used as an electrolyte. Ionic liquids are salts in liquid state at ambient temperature.[110] They present large electrochemical windows, high ionic conductivity, do not require the use of any additional solvent, are nonvolatile but also nonflammable.[111] They were

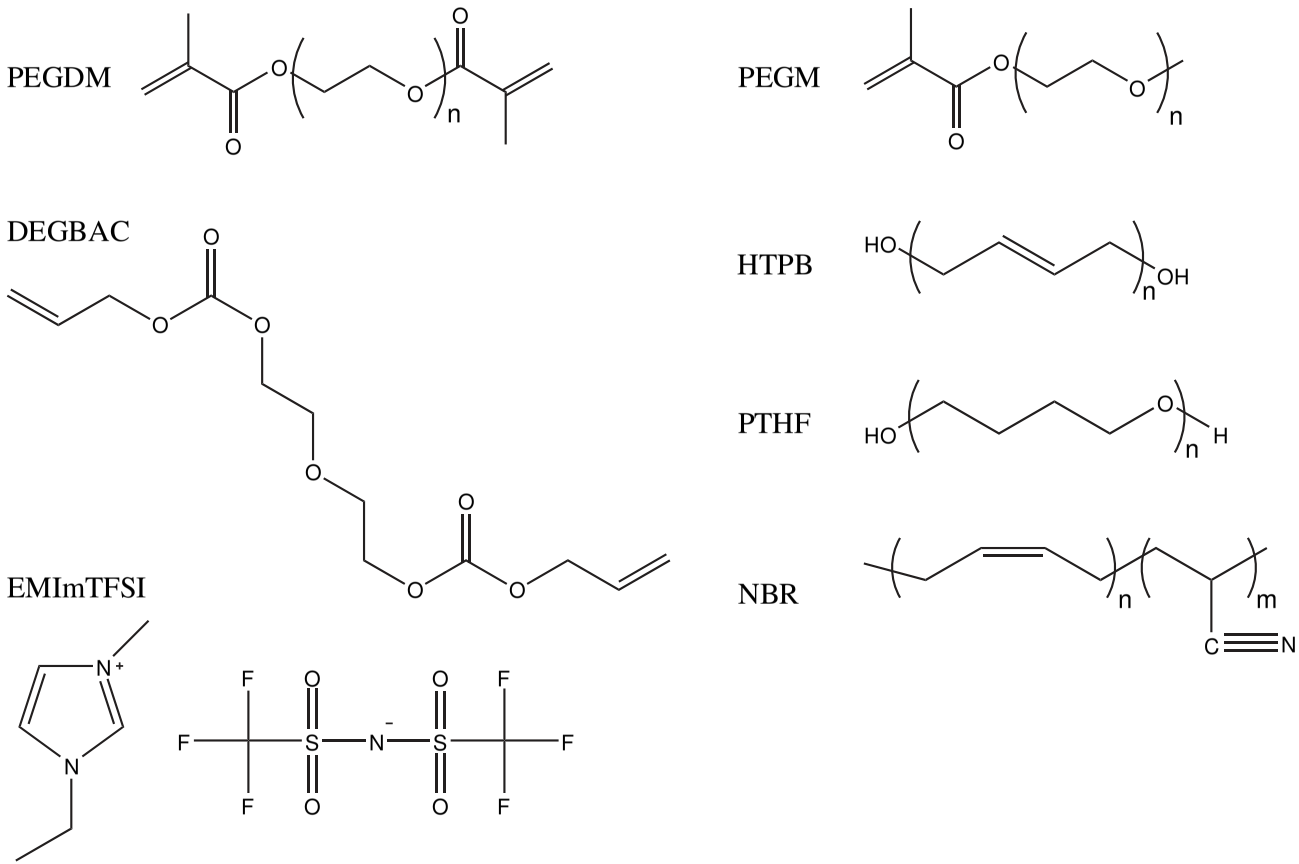

Scheme 12.2 Chemical structures of PEGDM, PEGM, DEGBAC, HTPB, PTHF, NBR and EMImTFSI ionic liquid.

described for the first time in 2002 by Lu *et al.* as electrolytes for π-conjugated polymer electrochemical devices with an enhanced lifetime (up to 1 million cycles).[89] In 2003, ionic liquids were used in actuator application for linear systems operating in solution[112] and for open-air bending trilayers.[90] Since then, many systems have been described and demonstrated high lifetime of the resulting actuators.[113]

The second issue was related to the delamination occurring at the interfaces of the layers due to the repeated electromechanical deformation of ECP electrodes. This problem has been solved thanks to several approaches at the same period as the introduction of ionic liquids. First, as mentioned earlier, the use of microporous PVdF membranes helped to improve the anchoring of the ECP layers on the central membrane.[90] For instance, Zhou *et al.* electropolymerized Py onto previously platinized commercial PVdF membrane.[90] Combined with the use of ionic liquids, the resulting PPy/PVdF/PPy trilayer actuators demonstrated 90° bending to either side and exceeded more than 3600 cycles without any obvious delamination between the electroactive PPy and the platinized PVdF layers. The use of commercially available PVdF membranes with defined thickness and dimensions may limit the possibility of tuning the geometry and performances of the resulting actuators. To overcome these issues, Gaihre *et al.* demonstrated the possibility to control the porosity and final thickness of homemade PVdF membrane for actuator applications.[114]

The delamination problem of the layers was also solved according to another approach by the synthesis of conducting IPNs (C-IPNs).[44,104,113,115] Instead of depositing the ECP layer on top of already fabricated membrane, ECP layers are interpenetrated within the membrane with their concentration decreasing from the surface to the central part of the film. Providing that no electrical connection occurs between the two electrodes, one-piece pseudo-trilayers are obtained, resolving de facto any delamination problem. This 3D interface, compared to the 2D interface of classical trilayer systems, may also improve the charge exchanges between the ECP electroactive layers and the ion reservoir membrane. Interpenetration of the electrodes was realized by chemical oxidative polymerization of EDOT with 1.5 M $FeCl_3$ aqueous solution in two steps. First, the EDOT monomers are introduced in the membrane by swelling and the resulting swollen membrane is immersed in oxidant solution. Due to opposite diffusion processes, *i.e.*, desorption of the EDOT from the membrane and absorption of the oxidant in the membrane, polymerization occurs within the surface of the membrane, resulting in the expected pseudo-trilayer configuration (see Figure 12.8).

The first C-IPN actuators, operating in open air, were introduced by the LPPI group in 2002, but a short life time was reported due to the appearance of cracks during bending deformation.[91] In this case, the ion reservoir membrane was already an IPN combining PEO network and polycarbonate (PC) network, as mentioned earlier, the interpenetrated ECP electrodes were made of PEDOT and the electrolyte was $LiClO_4/H_2O$. The brittleness of these first C-IPN actuators was solved by the synthesis of robust ionic membranes, and more

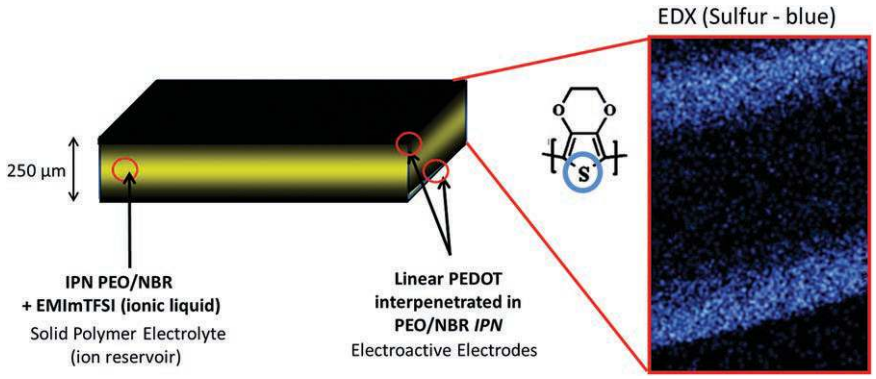

Figure 12.8 Conducting interpenetrating polymer network (C-IPN): schematic view of the configuration and EDX mapping of sulphur (blue) corresponding to PEDOT. In this example, the ion reservoir membrane displays an IPN macromolecular architecture with a total thickness of *ca.* 250 µm.

specifically by replacing the vitreous PC network by short-chain elastomer networks, such as PB[113,116] and PTHF[106] or by a second PEO network.[117] The synthesis of C-IPNs has also been described from a single network of high-molecular-weight rubber, such as NBR[97,98] and by PEO/NBR IPNs.[108] With the use of ionic liquids, strains up to 2.4% under ± 2.0 V, forces in the range of tens of mN (depending on device dimensions) and long life time (up to 7×10^6 cycles at a frequency of 10 Hz) have been obtained. It is also interesting to mention that the C-IPN architecture provides a control on the mechanical and electromechanical properties of the electrodes. Indeed, ECP chains are surrounded by other macromolecular chains in C-IPNs. As a consequence, a modification of ECP local concentration in the electrodes[118] or the introduction of another polymer partner[119] appears as a powerful tool for tuning the Young's modulus and the volumetric charge density of the electrodes, in order to control the final performances of the devices.

12.4 Electronically Conducting Polymer Microactuators

Electronically conducting polymer-based microactuators are promising candidates to enable a broad range of applications for new generation of soft microsystems where large strains are required. The concept and possible designs of microelectromechanical actuators based on ECPs were first described by Baughman in 1991.[120] He conceptually analyzed material properties and device designs based on experimental verifications on a macroscale to propose different approaches for fabricating ECP micro-actuators. Then, the combination of different microfabrication technologies (photolithography, etching techniques, metal deposition methods and laser ablation) allowed the design and fabrication of conducting polymer-based microsystems with a variety of configurations for different purposes.

The next subsections will give an overview of ECP microactuators based on their operation environment (in electrolytic solution and in open air).

12.4.1 Microactuators Operating in an Electrolytic Solution

The first microactuators were developed in bilayer configuration and operated in electrolytic solution. Smela *et al.* reported a work on bilayer strips of gold (Au) and dodecylbenzenesulphonate (DBS)-doped polypyrrole (PPy) in 1993.[71] They used standard photolithography of positive photoresist S1828 to fabricate millimetre-scale polymer fingers. After the dissolution of a sacrificial layer, the polymer fingers were connected to the Si wafer at one end but were free for the movement at the other. These fingers were stimulated in 0.1 M NaDBS aqueous solution and resulted in curling and uncurling with a response time of approximately 5 seconds. The same authors presented the possibility of a more complex configuration by combining the same DBS-doped PPy and Au bilayers with stiff parts.[82] The realization of these devices was done by combining standard photolithography, wet chemical etching and reactive ion etching (RIE). This work also demonstrated the differential adhesion method to release the bilayers by pulling themselves from the substrate when the electrical stimulation was applied. These microactuators with rigid elements had a configuration of an unfolded box. During electrical stimulation in NaDBS solution, the bilayer hinges achieved 180° bending, allowing the planar configuration microsystem to fold into an octahedron configuration (see Figure 12.9). Smela continued the research and demonstrated the fabrication of microsystems with a different release method.[121] The microactuator was fabricated using many different microfabrication technologies with the combination of standard photolithography, RIE, wet chemical etching, chemical vapour deposition (CVD) and metal evaporation. The novelty of this fabrication method was the release of the microsystems by finally etching through the Si wafer. These microsystems were electrically stimulated in NaDBS solution and the PPy/Au bilayer hinges were capable of lifting and positioning rigid Si and benzocyclobutene (BCB) plates.

Figure 12.9 Octahedron of PPy/Au bilayer hinge microactuators with rigid elements by M. Krogh *et al.*, Micromuscle AB, inspired by Smela *et al.*[82]
Reproduced from ref. 122 with permission from Elsevier, Copyright 2007.

Jager *et al.* demonstrated the fabrication of different microstructures for different purposes. They fabricated on-chip microsystems based on moveable PPy/Au bilayers with all the necessary electrodes (working, counter and reference) directly on a chip.[123] They found that the speed of the microactuators was the same compared to the usual device where macroscale electrodes were used. The next work proposed more complex design of a micro robot arm, consisting of an elbow, a wrist and a hand with fingers.[72] The joint parts were made of PPy/Au bilayers that were connected to stiff elements of benzocyclobutene (BCB). Different joints were stimulated separately, allowing the microarm to move, to grab and lift a 100 μm glass bead and to move it over a distance of 200–50 μm. The design and operation ability in different environments (salt solutions, blood plasma, urine and cell culture medium) make them attractive for biomedical applications. Over the years they reported studies on different designs of microstructures as microfluidic system, cell clinic and microactuators for different biomedical applications.[12,124–126]

A relatively simpler procedure of a PEDOT:PSS-based bilayer microactuator was proposed by Taccola *et al.*[127] The PEDOT:PSS/SU-8 bilayers with a final thickness of less than 600 nm (PEDOT:PSS 220 nm and SU-8 340 nm) were constructed by standard photolithography of SU-8 and wet chemical etching of PEDOT:PSS. The contacts were also included in the system but with manual wiring, after the fabrication of the microstructures. The system consisted of many fingers, which were stimulated at the same time in NaDBS aqueous solution and resulted in displacement from 220 to 2090 μm.

These bilayers have been integrated into complex microsystems for various applications over the past few decades. The operation in liquid electrolyte, especially in salt solutions, blood plasma, urine and cell culture medium, is mostly advantageous for biological and biomedical applications. In order to broaden the application field, the microactuator needs to be able to operate in open air. As mentioned earlier, for operation in the open air, the actuator needs to have a trilayer configuration with two electroactive electrodes sandwiching an ion storage membrane.

12.4.2 Microactuators Operating in the Open Air

The first air-operating microactuator was demonstrated by Alici *et al.* in 2009.[128] The microactuator was fabricated as a conventional macroscale actuator using a commercial PVdF membrane with a thickness of 110 μm and electropolymerizing PPy electrodes on both sides of the Au-coated PVdF membrane. The downscaling of the device was performed using a laser ablation technique, resulting in microactuators with dimensions 799×217×155 μm (length×width×thickness). Gaihre *et al.* presented the synthesis of PVdF thin films in order to decrease the final thickness of these PPy microactuators to 54 μm.[129] After synthesizing thinner PVdF films, they found that the actuator (850×250×54 μm) with PVdF membrane containing 0.05 M LiTFSI resulted in the highest tip displacement of 0.253 mm.[114] They also demonstrated that miniaturization of the actuators resulted in higher

strain energy per unit of mass or volume.[130] These trilayer microactuators were simple and obtained by a laser ablation technique or by manually cutting, later operated in the same manner as macroscale actuators, manually connecting the PPy microactuators to the macroscopic power supply.

Using similar PPy-Au-PVdF-based trilayer actuators, Jager *et al.* proposed a method to fabricate individually controllable actuators on a commercial flexible printed circuit board (FPCB).[131] The fabrication of the millimetre-scale actuators involved patterning of the Au on both faces of the PVdF membrane by flipping the substrate using wet chemical etching. Subsequently, the PPy electrodes were electropolymerized on the Au patterns simultaneously, resulting in trilayer actuators. The interface was fabricated separately and manually connected later with the resulting actuators. The actuators, 9 mm long and 2 mm wide, with FBCB interfacing, resulted in 18 mm tip displacement when stimulated under 1.5 V.

Another actuator composition and microfabrication method were proposed by Khaldi *et al.*[132,133] The microactuator was fabricated as a C-IPN composed of PEO/PTHF IPN as the ion reservoir membrane and PEDOT as interpenetrated electrodes. The low thickness of the resulting trilayer actuator (12 μm) allowed the use of RIE for patterning the actuators. The trilayer structure was manually placed on a PVA sacrificial layer in order to maintain it fixed and planar during the etching process, using photoresist as a mask. After the etching, microbeams were swollen in ionic liquid EMImTFSI before characterization. The microbeams with dimensions of 900×300×17 μm resulted in a large displacement amplitude of 950 μm, corresponding to the strain of 1.1%. The same authors optimized the thickness of these actuators and glued SU-8 parts on the microbeams to mimic the wings of a crane fly.[134] This work demonstrated improvement of the actuation frequency of 50 Hz, compared to the previous 0.05 Hz.

A further decrease of the thickness was demonstrated by Maziz *et al.* by the fabrication of C-IPN-based trilayer microactuators with an interpenetrating polymer network of PEO and nitrile butadiene rubber (NBR).[135,136] The PEDOT electrodes were here also obtained through chemical oxidative polymerization on both sides of the PEO/NBR layer. The involvement of a spin-coating step into the fabrication process allowed tuning of the thickness of the membrane layer from 600 nm to 30 μm. The actuators were patterned using standard photolithography and RIE, resulting in microactuators with final thicknesses of 6, 12 and 19 μm. These microactuators demonstrated strain differences up to 0.9% and output forces in the range of μN. More importantly, reducing the final thickness of the microactuators allowed demonstrating actuation at a high resonant frequency of 930 Hz.

Recently, another interesting work was demonstrated by Khaldi *et al.* about patterning techniques for conducting polymers.[137] They presented two patterning methods: micro-contact printing (μCP) and syringe-based printing. The PDMS stamp was used for μCP, where an oxidant solution layer was deposited through the stamp on PVdF membrane and followed by the vapour phase polymerization (VPP) of EDOT, resulting in well-defined micropatterned electrodes. The PDMS stamp and μCP allow patterning of the device architecture in

a single step with individually controllable actuators, wires and contact pads. Unfortunately, they did not succeed in using this technique on PEO-NBR membrane due to the insufficient affinity between the oxidant solution and the PEO-NBR membrane. Consequently, they used the second patterning method. Syringe-based printing requires different affinity and the PEO-NBR membrane was found to be suitable for this process. They fabricated the trilayer actuator based on a layer-stacking method. First, an oxidant solution was deposited in the desired shape using syringe-based printing followed by the EDOT VPP. The PEO-NBR network precursors were deposited through spin-coating, followed by a short curing and the second electrode was obtained in the same way as the first one. The final systems were cut out from the membrane using laser ablation and fabricated milli/micro hand actuator resulting in a 2.2% strain difference, stimulated at ± 2.0 V with a thickness of 70 μm. This work proposed printing methods that have not been used so far for microactuator fabrication. Nonetheless, electrical connections were not integrated to the system requiring the use of macroscopic connections to electrically stimulate the resulting microactuators.

Except the work of Jager, all reported attempts on air-operated microactuators have been reported without the integration of electrical connections. As said earlier, in order to fabricate an efficient microsystem, electrical contacts have to be integrated in the system, and ideally directly during its fabrication, to connect the actuator with an electrical supply. For this purpose, Khaldi *et al.* proposed a bottom-up process to fabricate a system with individual control of the system.[138,139] The process combined standard photolithography, wet chemical etching, evaporation and sputtering. The reported work proposed a fabrication of millimetre-scale actuators, resulting in a relatively low strain of 0.01% at ± 1.0 V. Even though the fabrication process was successful and two electrical connections were incorporated, the final samples were manually cut out of the substrate, which makes it harder to manipulate, if the sample dimensions are decreased.

On the other hand, Maziz *et al.* reported a microactuator fabrication method on a flexible substrate, called the top-down approach.[140] This process is the first to integrate one electrical connection into an open-air actuating microdevice without any kind of manual handling, using different microsystem technologies. The realization of the trilayer actuator was performed using a layer-stacking method, *i.e.*, by sequentially stacking layers on top of the previous layers. Using spin-coating to deposit the layers allows precise control over the thickness of each layer and allows the fabrication without any manual handling during the synthesis. The PEDOT electrodes were obtained through EDOT vapour phase polymerization (VPP) and the membrane layer through radical polymerization of spin-coated PEO-NBR solution precursors. The PEDOT/PEO-NBR/PEDOT trilayer microactuators were fabricated on a SU-8 substrate with bottom electrical contact by combining standard photolithography, evaporation and RIE (see Figure 12.10). The second contact was obtained by placing a micromechanical gold tip on top of the trilayer. The microactuator ($650 \times 100 \times 10$ μm) was electrically

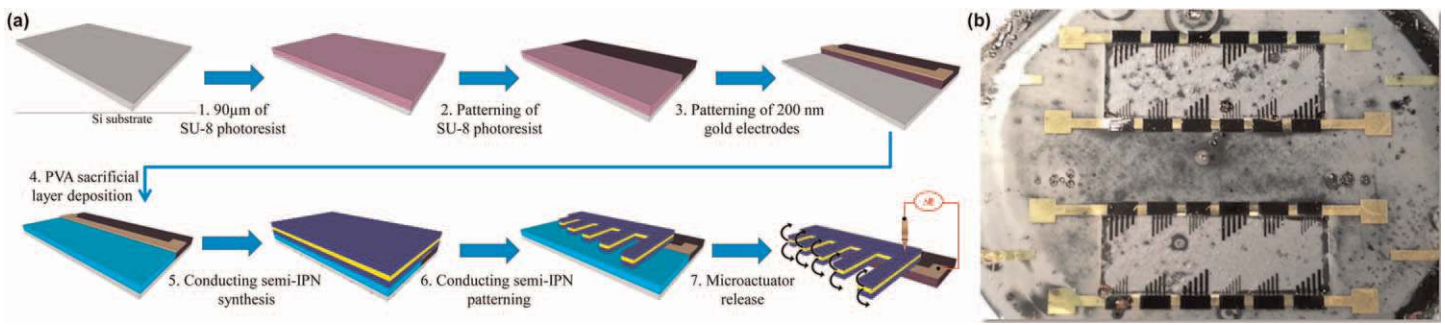

Figure 12.10 (a) Overview of the fabrication steps and (b) photograph of the microactuators fabricated with the layer-stacking method and with integrated bottom electrical contact.
Reproduced from ref. 140 with permission from the American Chemical Society, Copyright 2016.

stimulated in air (±4.0 V) and resulted in a strain difference of 0.13% and an output force of 0.75 μN. This work presented a great improvement compared to previous works with full integration of bottom electrical contact and subsequent operation on a soft substrate and resulted in a functioning microactuator after all the microfabrication processing steps. The disadvantage of this method remains in the absence of the second electrical contact from the top of the PEDOT electrode, requiring manual connection of this electrode for the characterization and relatively low performances.

More recently, Zhong *et al.*[141] demonstrated the fabrication of a photopatternable ionic reservoir membrane composed of bisphenol A ethoxylate dimethacrylate (BEMA) and poly(ethylene glycol) methyl ether methacrylate (PEGMA) networks with the necessary ions for the redox process directly incorporated before the photopolymerization. The microsystem was realized by locally electropolymerizing PPy electrodes in photoresist holes on a gold-coated wafer. Subsequently, the membrane was micropatterned locally on top of the PPy layer using photolithography, resulting in bilayer microactuators. The final release was performed by wet chemical etching to form the device layout. After the etching, the working electrodes were movable but still attached to the wafer. The final microdevice was fabricated with parallel electrode configuration. In this case, the working and counter electrodes were placed parallel under the actuator, between which the ions were shuttled during the electrical stimulation (see Figure 12.11). This novel method and the development of the photopatternable ionogel would be advantageous for microstructure fabrication. Although the novel fabrication method was reported, the performances of the actuators were almost nonexistent, probably due to the low ionic conductivity of the BEMA gel after all the processing steps.

Finally, Plesse *et al.* described the synthesis of trilayer microactuators and microsensors fully compatible with microsystem processes and with integrated electrical connections. Commercially available poly(3,4-ethylenedioxythiophene):poly(styrene sulphonate) (PEDOT:PSS) dispersion was chosen as an electrode material for the fabrication of microactuators. The poor electrical, mechanical and electrochemical properties of pristine PEDOT:PSS electrodes were improved significantly by formulation of the commercial dispersion with polar reactive additive based on methacrylic poly(ethylene glycol) and its subsequent polymerization within the PEDOT:PSS material leading to a PEDOT:PSS:PEO electrode. The synthesis of PEDOT:PSS:PEO trilayers was performed according to the layer stacking method (see Figure 12.12a). Patterning was performed first by laser ablation to obtain PEDOT:PSS-based microactuators. While electrically connected manually, these PEDOT:PSS/PEO microactuators presented high performances with a maximum strain of 0.82% and maximum output force of 472 μN under ±2.2 V (see Figure 12.12b).[142] More importantly, the mechanical sensing behaviour was demonstrated for the first time at the microscale and presented enhancement of the sensitivity compared to the macroscale ECP-based actuators (maximum output voltage 0.42 mV at 0.5% strain). The full microsystem process was then performed to integrate such electroactive

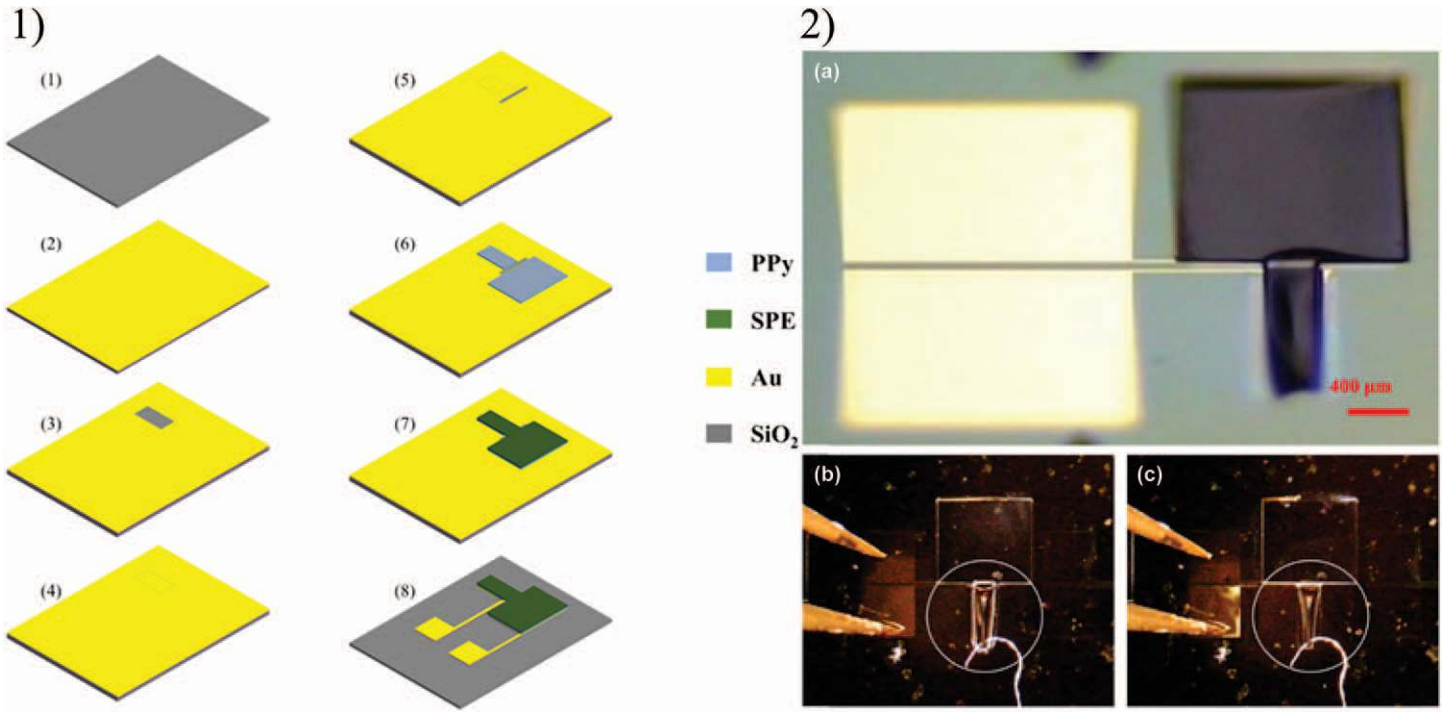

Figure 12.11 Solid-state polypyrrole microactuator: (1) overview of the fabrication steps and (2) photographs of the microactuator, (a) as fabricated, (b) and (c) actuation results showing folding motion.
Reproduced from ref. 141, https://doi.org/10.1088/1361-665X/aabe42, under the terms of the CC BY 3.0 licence, https://creativecommons.org/licenses/by/3.0/.

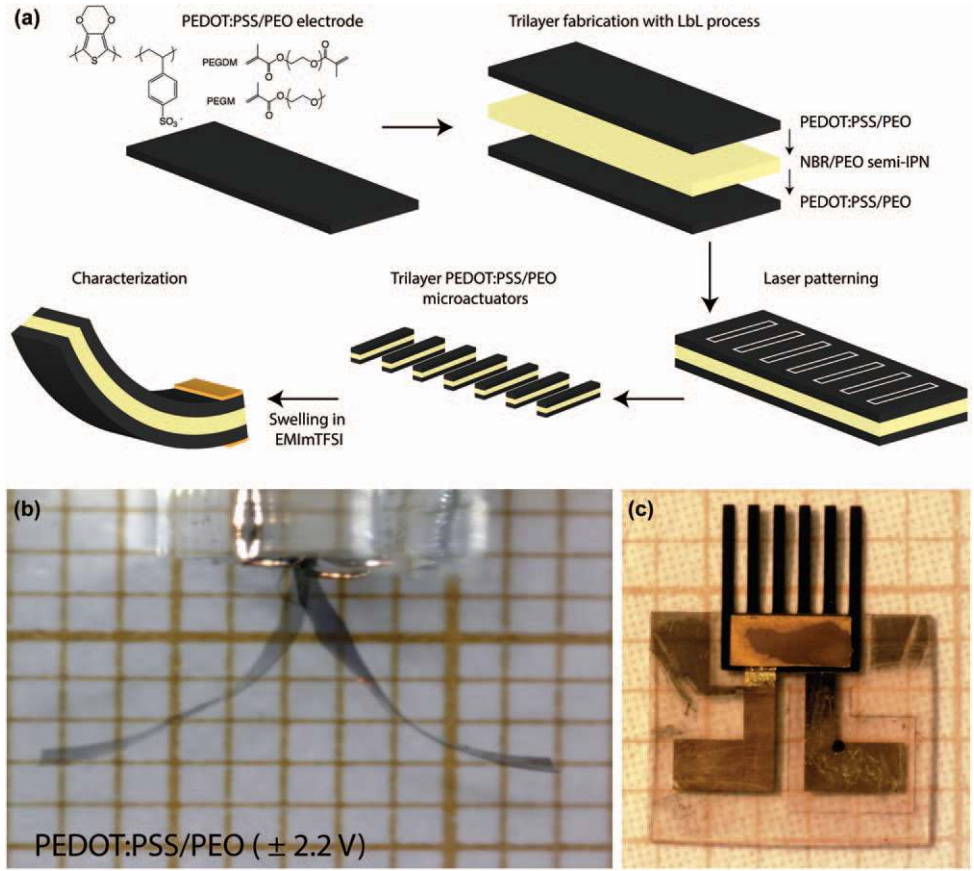

Figure 12.12 (a) PEDOT:PSS/PEO microactuator fabrication with the layer-stacking method; (b) PEDOT:PSS/PEO microactuator under electrical stimulation of ±2.2 V; (c) fully integrated PEDOT:PSS/PEO microsystem with two electrical contacts directly on a flexible substrate.
Part (a) reproduced from ref. 142 with permission from John Wiley and Sons, © 2019 Wiley-VCH Verlag GmbH & Co. KGaA, Weinheim.

microdevices into microsystems with two electrical contacts directly on a flexible substrate (see Figure 12.12c).[143] The microfabrication process was realized by combining different microfabrication technologies (photolithography, etching, metal evaporation) and the microsystems were developed by reversing the steps, *i.e.*, fabricating the microactuators first and finally encapsulating them into SU-8 to obtain the flexible support. The resulting process allows the fabrication of microsystems with different configurations and designs, for example, the realization of the actuator-sensor microsystem with two separate pairs of electrical contacts. The resulting microsystems demonstrated a maximum strain of 0.66% and maximum output force of 105 μN under ±3.0 V. Additionally, the mechanical sensing behaviour was demonstrated for the first time for microsystems with integrated electrical contacts, resulting in a maximum output voltage of 0.35 mV at 0.34% strain. In other words, this electromechanical ECP microdevice is to date the closest demonstration of air-operating soft MEMS based on ECPs and theoretically ready for further integration into complex systems.

12.5 Conclusions and Perspectives

This chapter depicted the state of the art in the field of conducting polymers as redox materials for the development of soft microelectromechanical systems. This multidisciplinary field gathers polymer and material chemistry, electrochemistry, physics, microfabrication and engineering. While impressive and eye-catching demonstrators have been proposed 20 years ago on "in-electrolyte" operation, still suitable for biology-related applications, it took the efforts of numerous groups to push this technology forward and demonstrate it in the open air. Integrated and soft microactuators/microsensors have been finally demonstrated and are now opening promising perspectives for applications in soft electronics and microelectronics. Among others, the development of open-air microgrippers with haptic feedback can now be explored where interfaced microactuators and microsensors acting as finger, wrist and elbow may allow grabbing and "feeling" micro-objects. Micropatterned sheets with bumping area can be also envisioned for texturing the surfaces of smart screens (phone, TV, cars) or for the development of soft, light, rollable and refreshable braille displays. Integration of micromuscle to actuate flapping wings or legs also makes the development of a scale-1 microdrone mimicking fly or crawling insects one step closer.

However, several challenges and issues remain. The "wet" nature of these materials, requiring the presence of an ionic conducting phase, may cause evaporation and leaking issues. Ionic liquid electrolyte could overcome the evaporation issue, nevertheless the electrolyte leaking can be a major drawback if these devices are to be used for medicinal purposes. A solution could come from the development of "dry" ionic devices by the use of polymeric ionic liquids. These materials are a sub-class of polyelectrolyte bearing ionic liquid-type functions along their polymer backbones. They can then bring together the best of both worlds, *i.e.*, ionic conductivity of ionic liquids and mechanical properties of polymers. Unfortunately, to date, their ionic conductivity remains low compared to the corresponding ionic liquids,

and any further improvement is usually at the expense of the mechanical properties, critical for electromechanical applications. Another question, common with all of the new soft organic electronics, is related to the end-of-life. While bio-based and biodegradable membranes and bio-compatible ionic liquids are widely studied nowadays, the possibility to synthesize efficient and (bio-)degradable conducting polymers remains a hurdle. Blending with bio-degradable compounds is of course an identified and studied path, but the development of truly (bio-)degradable conjugated and electrically conducting polymer chains will require the efforts of chemists in the next decade to allow these materials to develop their full potential while respecting the necessary constraints of an environmentally responsible (friendly) world.

References

1. Y. Bar-Cohen, in *SPIE EAPAD*, San Diego, California, March, 2005.
2. Y. Bar-Cohen, *Electroactive Polymer (EAP) Actuators as Artificial Muscles: Reality, Potential, and Challenges, SPIE – The International Society for Optical Engineering*, 2nd edn, Washington, 2004.
3. R. Pelrine, R. Kornbluh, Q. Pei and J. Joseph, *Science*, 2000, **287**, 836–839.
4. H. S. Nalwa, *Ferroelectic Polymers – Chemistry, Physics and Applications*, Marcel Dekker, Inc., New York, 1995.
5. V. D. Kugel, B. Xu, Q. M. Zhang and L. E. Cross, *Sens. Actuators, A*, 1998, **69**, 234–242.
6. J. Y. Li and N. Rao, *J. Mech. Phys. Solids*, 2004, **52**, 591–615.
7. X. Ji, A. El Haitami, F. Sorba, S. Rosset, G. T. M. Nguyen, C. Plesse, F. Vidal, H. R. Shea and S. Cantin, *Sens. Actuators, B*, 2018, **261**, 135–143.
8. R. H. Baughman, *Makromol. Chem., Mocromol. Symp.*, 1991, **51**, 193–215.
9. Y. Osada and J. Gong, *Prog. Polym. Sci.*, 1993, **18**, 187–226.
10. P. Calvert, J. O'Kelly and C. Souvignier, *Mater. Sci. Eng., C*, 1998, **6**, 167–174.
11. R. H. Baughman, *Synth. Met.*, 1996, **78**, 339–353.
12. E. W. H. Jager, E. Smela and O. Inganäs, *Science*, 2000, **290**, 1540–1545.
13. M. Shahinpoor, Y. Bar-Cohen, O. J. Simpson and J. Smith, *Smart Mater. Struct.*, 1998, **7**, R15.
14. R. H. Baughman, C. Cui, A. A. Zakhidov, Z. Iqbal, J. N. Barisci, G. M. Spinks, G. G. Wallace, A. Mazzoldi, D. De Rossi, A. G. Rinzler, O. Jaschinski, S. Roth and M. Kertesz, *Science*, 1999, **284**, 1340–1344.
15. T. Sugino, K. Kiyohara, I. Takeuchi, K. Mukai and K. Asaka, *Sens. Actuators, B*, 2009, **141**, 179–186.
16. I. Takeuchi, K. Asaka, K. Kiyohara, T. Sugino, N. Terasawa, K. Mukai, T. Fukushima and T. Aida, *Electrochim. Acta*, 2009, **54**, 1762–1768.
17. R. Dash, J. Chmiola, G. Yushin, Y. Gogotsi, G. Laudisio, J. Singer, J. Fischer and S. Kucheyev, *Carbon N. Y.*, 2006, **44**, 2489–2497.
18. J. Torop, M. Arulepp, J. Leis, A. Punning, U. Johanson, V. Palmre and A. Aabloo, *Materials*, 2010, **3**, 9–25.
19. H. Shirakawa, E. J. Louis, S. C. Gau, A. G. MacDiarmid, C. K. Chiang, C. R. Fincher, Y. W. Park and A. J. Heeger, *Phys. Rev. Lett.*, 1977, **39**, 1098–1101.

20. A. J. Heeger, A. G. MacDiarmid and H. Shirakawa, *Nobel Prize Chemistry, 2000 Conductive Polymers*, Royal Swedish Academy of Sciences, Stockholm, Sweden, 2000.
21. A. G. MacDiarmid, *Synth. Met.*, 2002, **125**, 11–22.
22. J. L. Brédas, J. C. Scott, K. Yakushi and G. B. Street, *Phys. Rev. B*, 1984, **30**, 1023–1025.
23. J. L. Brédas and G. B. Street, *Acc. Chem. Res.*, 1985, **18**, 309–315.
24. T. C. Chung, J. H. Kaufman, A. J. Heeger and F. Wudl, *Phys. Rev. B*, 1984, **30**, 702–710.
25. H. Naarmann and N. Theophilou, *Synth. Met.*, 1987, **22**, 1–8.
26. P. N. Adams, P. Devasagayam, S. J. Pomfret, L. Abell and A. P. Monkman, *J. Phys.: Condens. Matter*, 1998, **10**, 8293–8303.
27. Y. Nogami, J. P. Pouget and T. Ishiguro, *Synth. Met.*, 1994, **62**, 257–263.
28. R. D. McCullough, S. P. Williams, R. D. Lowe, M. Jayaraman and S. Tristram-Nagle, *J. Am. Chem. Soc.*, 1993, **115**, 4910–4911.
29. B. Winther-Jensen, D. W. Breiby and K. West, *Synth. Met.*, 2005, **152**, 1–4.
30. M. R. Gandhi, P. Murray, G. M. Spinks and G. G. Wallace, *Synth. Met.*, 1995, **73**, 247–256.
31. Q. Pei and O. Inganäs, *Solid State Ionics*, 1993, **60**, 161–166.
32. T. F. Otero, H. Grande and J. Rodriguez, *J. Phys. Org. Chem.*, 1996, **9**, 381–386.
33. Y. Qiu and J. R. Reynolds, *Polym. Eng. Sci.*, 1991, **31**, 417–421.
34. C. Lopez, M. F. M. Viegas, G. Bidan and E. Vieil, *Synth. Met.*, 1994, **63**, 73–78.
35. Q. Pei and O. Inganäs, *J. Phys. Chem.*, 1992, **96**, 10507–10514.
36. T. Matencio, M. A. De Paoli, R. C. D. Peres, R. M. Torresi and S. I. Cordoba de Torresi, *Synth. Met.*, 1995, **72**, 59–64.
37. R. Temmer, A. Maziz, C. Plesse, A. Aabloo, F. Vidal and T. Tamm, *Smart Mater. Struct.*, 2013, **22**, 1–16.
38. Y. Sonoda, W. Takashima and K. Kaneto, *Synth. Met.*, 2001, **119**, 267–268.
39. B. Qi, W. Lu and B. R. Mattes, *J. Phys. Chem. B*, 2004, **108**, 6222–6227.
40. H. Okuzaki, T. Kondo and T. Kunugi, *Polymer*, 1999, **40**, 995–1000.
41. J. D. W. Madden, PhD thesis Massachusetts Inst. Technol., 2000.
42. A. Elschner, S. Kirchmeyer, W. Lövenich, U. Merker and K. Reuter, *PEDOT – Principles and Applications of an Intrinsically Conductive Polymer*, Taylor & Francis Group, Boca Raton, 2011.
43. R. Temmer, I. Must, F. Kaasik, A. Aabloo and T. Tamm, *Sens. Actuators, B*, 2012, **166–167**, 411–418.
44. F. Vidal, J. F. Popp, C. Chevrot and D. Teyssié, *Smart Struct. Mater. 2002 Electroact. Polym. Actuators Devices*, 2002, **4695**, 95–103.
45. A. Mohammadi, M. A. Hasan, B. Liedberg, I. Lundström and W. R. Salaneck, *Synth. Met.*, 1986, **14**, 189–197.
46. L. Groenendaal, F. Jonas, D. Freitag, H. Pielartzik and J. R. Reynolds, *Adv. Funct. Mater.*, 2000, **12**, 481–494.
47. Y. Wang, C. Zhu, R. Pfattner, H. Yan, L. Jin, S. Chen, F. Molina-Lopez, F. Lissel, J. Liu, N. I. Rabiah, Z. Chen, J. W. Chung, C. Linder, M. F. Toney, B. Murmann and Z. Bao, *Sci. Adv.*, 2017, **3**, 1–10.

48. T. A. Skotheim and J. R. Reynolds, *Conjugated Polymers, Theory, Synthesis, Properties, and Characterization*, 3rd edn, Taylor & Francis Group, Boca Raton, 2007.
49. F. Louwet, L. Groenendaal, J. Dhaen, J. Manca, J. Van Luppen, E. Verdonck and L. Leenders, *Synth. Met.*, 2003, **135–136**, 115–117.
50. N. Kim, S. Kee, S. H. Lee, B. H. Lee, Y. H. Kahng, Y. R. Jo, B. J. Kim and K. Lee, *Adv. Mater.*, 2014, **26**, 2268–2272.
51. Y. Xia, K. Sun and J. Ouyang, *Adv. Mater.*, 2012, **24**, 2436–2440.
52. M. Cai, Z. Ye, T. Xiao, R. Liu, Y. Chen, R. W. Mayer, R. Biswas, K. M. Ho, R. Shinar and J. Shinar, *Adv. Mater.*, 2012, **24**, 4337–4342.
53. Z. Zhao, G. F. Richardson, Q. Meng, S. Zhu, H. C. Kuan and J. Ma, *Nanotechnology*, 2016, **27**, 42001.
54. H. Yan, T. Jo and H. Okuzaki, *Polym. J.*, 2009, **41**, 1028–1029.
55. H. Okuzaki, H. Suzuki and T. Ito, *Synth. Met.*, 2009, **159**, 2233–2236.
56. A. Simaite, B. Tondu, P. Souères and C. Bergaud, *ACS Appl. Mater. Interfaces*, 2015, **7**, 19966–19977.
57. A. Simaite, F. Mesnilgrente, B. Tondu, P. Souères and C. Bergaud, *Sens. Actuators, B*, 2016, **229**, 425–433.
58. I. Põldsalu, K. Rohtlaid, T. Minh, G. Nguyen, C. Plesse, F. Vidal, M. S. Khorram, A. Peikolainen, T. Tamm and R. Kiefer, *Sens. Actuators, B*, 2018, **258**, 1072–1079.
59. J. Huang, P. F. Miller, J. C. De Mello, A. J. De Mello and D. D. C. Bradley, *Synth. Met.*, 2003, **139**, 569–572.
60. A. Moujoud, S. H. Oh, H. S. Shin and H. J. Kim, *Phys. Status Solidi Appl. Mater. Sci.*, 2010, **207**, 1704–1707.
61. J. Y. Kim, J. H. Jung, D. E. Lee and J. Joo, *Synth. Met.*, 2002, **126**, 311–316.
62. C. Badre, L. Marquant, A. M. Alsayed and L. A. Hough, *Adv. Funct. Mater.*, 2012, **22**, 2723–2727.
63. B. Fan, X. Mei and J. Ouyang, *Macromolecules*, 2008, **41**, 5971–5973.
64. Y. Xia and J. Ouyang, *Org. Electron. physics, Mater. Appl.*, 2010, **11**, 1129–1135.
65. Y. Xia, H. Zhang and J. Ouyang, *J. Mater. Chem.*, 2010, **20**, 9740.
66. Y. Xia and J. Ouyang, *ACS Appl. Mater. Interfaces*, 2010, **2**, 474–483.
67. E. Dauzon, A. E. Mansour, M. R. Niazi, R. Munir, D. M. Smilgies, X. Sallenave, C. Plesse, F. Goubard and A. Amassian, *ACS Appl. Mater. Interfaces*, 2019, **11**, 17570–17582.
68. R. H. Baughman, L. W. Shacklette, R. L. Elsenbaumer, E. Plichta and C. Becht, *Conducting Polymer Electromechanical Actuators*, Kluwer Academic Publishers, Dordrecht, 1990.
69. P. Chiarelli, D. De Rossi, A. Della Santa and A. Mazzoldi, *Polym. Gels Networks*, 1994, **2**, 289–297.
70. M. Kaneko, M. Fukui, W. Takashima and K. Kaneto, *Synth. Met.*, 1997, **84**, 795–796.
71. E. Smela, O. Inganäs, Q. Pei and I. Lundström, *Adv. Mater.*, 1993, **5**, 630–632.

72. E. W. H. Jager, O. Inganäs and I. Lundström, *Science*, 2000, **288**, 2335–2338.
73. T. F. Otero and J. Rodríguez, *Intrinsically Conducting Polymers: An Emerging Technology*, 1992.
74. S. J. Higgins, K. V. Lovell, R. M. Gamini Rajapakse and N. M. Walsby, *J. Mater. Chem.*, 2003, **13**, 2485.
75. S. D. Deshpande, J. Kim and S. R. Yun, *Synth. Met.*, 2005, **149**, 53–58.
76. S. D. Deshpande, J. Kim and S. R. Yun, *Smart Mater. Struct.*, 2005, **14**, 876–880.
77. G. Alici, A. Punning and H. R. Shea, *Sens. Actuators, B*, 2011, **151**, 72–84.
78. T. F. Otero, E. Angulo, J. Rodríguez and C. Santamaría, *J. Electroanal. Chem.*, 1992, **341**, 369–375.
79. Q. Pei and O. Inganas, *Adv. Mater.*, 1992, **4**, 227–278.
80. T. F. Otero, J. M. Sansinena and J. M. Sansiñena, *Bioelectrochem. Bioenerg.*, 1995, **38**, 411–414.
81. M. Kaneko and K. Kaneto, *React. Funct. Polym.*, 1998, **37**, 155–161.
82. E. Smela, O. Inganäs and I. Lundström, *Science*, 1995, **268**, 1735–1738.
83. E. Smela, *J. Micromech. Microeng.*, 1999, **9**, 1–18.
84. M. Fuchiwaki and T. F. Otero, *J. Mater. Chem. B*, 2014, **2**, 1954–1965.
85. T. F. Otero and J. G. Martinez, *Sens. Actuators, B*, 2014, **199**, 27–30.
86. Q. Pei, O. Inganäs, G. Gustafsson and M. Granström, *Synth. Met.*, 1993, **55**, 1221–1226.
87. J. M. Sansinena, V. Olazabal, T. F. Otero, C. N. Polo da Fonseca and M. A. De Paoli, *Chem. Commun.*, 1997, **22**, 2217–2218.
88. T. W. Lewis, L. A. P. Kane-Maguire, A. S. Hutchison, G. M. Spinks and G. G. Wallace, *Synth. Met.*, 1999, **102**, 1317–1318.
89. W. Lu, A. G. Fadeev, B. Qi, E. Smela, B. R. Mattes, J. Ding, G. M. Spinks, J. Mazurkiewicz, D. Zhou, G. G. Wallace, D. R. MacFarlane, S. A. Forsyth and M. Forsyth, *Science*, 2002, **297**, 983–987.
90. D. Zhou, G. M. Spinks, G. G. Wallace, C. Tiyapiboonchaiya, D. R. MacFarlane, M. Forsyth and J. Sun, *Electrochim. Acta*, 2003, **48**, 2355–2359.
91. F. Vidal, J. F. Popp, C. Plesse, C. Chevrot and D. Teyssié, *J. Appl. Polym. Sci.*, 2003, **90**, 3569–3577.
92. M. Khayet and T. Matsuura, *Ind. Eng. Chem. Res.*, 2001, **40**, 5710–5718.
93. X. Wang, C. Xiao, H. Liu, Q. Huang and H. Fu, *J. Appl. Polym. Sci.*, 2018, **135**, 46711.
94. M. Qtaishat, T. Matsuura, B. Kruczek and M. Khayet, *Desalination*, 2008, **219**, 272–292.
95. G. Li, Z. Li, P. Zhang, H. Zhang and Y. Wu, *Pure Appl. Chem.*, 2008, **80**, 2553–2563.
96. X. Tang, R. Muchakayala, S. Song, Z. Zhang and A. R. Polu, *J. Ind. Eng. Chem.*, 2016, **37**, 67–74.
97. M. S. Cho, H. J. Seo, J. D. Nam, H. R. Choi, J. C. Koo, K. G. Song and Y. Lee, *Sens. Actuators, B*, 2006, **119**, 621–624.
98. M. S. Cho, H. J. Seo, J. D. Nam, H. R. Choi, J. C. Koo and Y. Lee, *Smart Mater. Struct.*, 2007, **16**, S237.

99. H. J. Choi, Y. M. Song, I. Chung, K. S. Ryu and N. J. Jo, *Smart Mater. Struct.*, 2009, **18**, 1–6.
100. Y. Li, R. Tanigawa and H. Okuzaki, *Smart Mater. Struct.*, 2014, **23**, 1–8.
101. H. Okuzaki, S. Takagi, F. Hishiki and R. Tanigawa, *Sens. Actuators, B*, 2014, **194**, 59–63.
102. L. H. Sperling, *Adv. Chem.*, 1994, **239**, 3–38.
103. A. D. Jenkins, P. Kratochvíl, R. F. T. Stepto and U. W. Suter, *Pure Appl. Chem.*, 1996, **68**, 2287–2311.
104. C. Plesse, F. Vidal, C. Gauthier, J. M. Pelletier, C. Chevrot and D. Teyssié, *Polymer*, 2007, **48**, 696–703.
105. C. Gauthier, C. Plesse, F. Vidal, J. M. Pelletier, C. Chevrot and D. Teyssié, *Polymer*, 2007, **48**, 7476–7483.
106. C. Plesse, A. Khaldi, Q. Wang, E. Cattan, D. Teyssié, C. Chevrot and F. Vidal, *Smart Mater. Struct.*, 2011, **20**, 1–8.
107. N. Festin, C. Plesse, P. Pirim, C. Chevrot and F. Vidal, *Sens. Actuators, B*, 2014, **193**, 82–88.
108. N. Festin, A. Maziz, C. Plesse, D. Teyssié, C. Chevrot and F. Vidal, *Smart Mater. Struct.*, 2013, **22**, 104005.
109. K. Kaneto, M. Kaneko, Y. Min and A. G. MacDiarmid, *Synth. Met.*, 1995, **71**, 2211–2212.
110. P. Bonhôte, A.-P. Dias, N. Papageorgiou, K. Kalyanasundaram and M. Grätzel, *Inorg. Chem.*, 1996, **35**, 1168–1178.
111. M. Galiński, A. Lewandowski and I. Stepniak, *Electrochim. Acta*, 2006, **51**, 5567–5580.
112. J. Ding, D. Zhou, G. Spinks, G. Wallace, S. Forsyth, M. Forsyth and D. MacFarlane, *Chem. Mater.*, 2003, **15**, 2392–2398.
113. F. Vidal, C. Plesse, D. Teyssié and C. Chevrot, *Synth. Met.*, 2004, **142**, 287–291.
114. B. Gaihre, G. Alici, G. M. Spinks and J. M. Cairney, *Sens. Actuators, B*, 2011, **155**, 810–816.
115. F. Vidal, C. Plesse, H. Randriamahazaka, D. Teyssie and C. Chevrot, *Mol. Cryst. Liq. Cryst.*, 2006, **448**, 95–102.
116. H. Randriamahazaka, C. Plesse, F. Vidal, C. Gauthier, C. Chevrot and D. Teyssie, *Smart Structures and Materials 2004: Electroactive Polymer Actuators and Devices*, 2004, **vol. 5385**, 294–301.
117. C. Plesse, F. Vidal, D. Teyssie and C. Chevrot, *Adv. Sci. Technol.*, 2008, **61**, 53–58.
118. A. Fannir, R. Temmer, G. T. M. Nguyen, L. Cadiergues, E. Laurent, J. D. W. Madden, F. Vidal and C. Plesse, *Adv. Mater. Technol.*, 2018, **1800519**, 1–8.
119. V. Woehling, G. T. M. Nguyen, C. Plesse, S. Cantin, J. D. W. Madden and F. Vidal, *Sens. Actuators, B*, 2018, **256**, 294–303.
120. R. H. Baughman, L. W. Shacklette, R. L. Elsenbaumer, E. J. Plichta and C. Becht, *Micro Electromechanical Actuators Based on Conducting Polymers*, Springer, Dordrecht, 1991.
121. E. Smela, M. Kallenbach and J. Holdenried, *J. Microelectromech. Syst.*, 1999, **8**, 373–383.

122. S. A. Wilson, R. P. J. Jourdain, Q. Zhang, R. A. Dorey, C. R. Bowen, M. Willander, Q. U. Wahab, M. Willander, S. M. Al-hilli, O. Nur, E. Quandt, C. Johansson, E. Pagounis, M. Kohl, J. Matovic, B. Samel, W. van der Wijngaart, E. W. H. Jager, D. Carlsson, Z. Djinovic, M. Wegener, C. Moldovan, E. Abad, M. Wendlandt, C. Rusu and K. Persson, *Mater. Sci. Eng. R Reports*, 2007, **56**, 1–129.
123. E. W. H. Jager, E. Smela and O. Inganäs, *Sens. Actuators, B*, 1999, **56**, 73–78.
124. P. F. Pettersson, E. W. H. Jager and O. Inganas, *1st Annu. Int. IEEE-EMBS Spec. Top. Conf. Microtechnologies Med. Biol. Proc.* (Cat. No.00EX451), 2000, **56**, 1999–2000.
125. E. W. H. Jager, C. Immerstrand, K. H. Peterson, K. E. Magnusson, I. Lundström and O. Inganäs, *Biomed. Microdevices*, 2002, **4**, 177–187.
126. C. Immerstrand, E. W. H. Jager, K.-E. Magnusson, T. Sundqvist, I. Lundström, O. Inganas and K. H. Peterson, *Med. Biol. Eng. Comput.*, 2003, **41**, 357–364.
127. S. Taccola, F. Greco, B. Mazzolai, V. Mattoli and E. W. H. Jager, *J. Micromech. Microeng.*, 2013, **23**, 117004.
128. G. Alici and M. J. Higgins, *Smart Mater. Struct.*, 2009, **18**, 065013.
129. B. Gaihre, G. Alici, G. M. Spinks and J. M. Cairney, *Sens. Actuators, A*, 2010, **165**, 321–328.
130. B. Gaihre, G. Alici, G. M. Spinks and J. M. Cairney, *J. Microelectromech. Syst.*, 2012, **21**, 574–585.
131. E. W. H. Jager, N. Masurkar, N. F. Nworah, B. Gaihre, G. Alici and G. M. Spinks, *Sens. Actuators, B*, 2013, **183**, 283–289.
132. A. Khaldi, C. Plesse, C. Soyer, E. Cattan, F. Vidal, C. Legrand and D. Teyssié, *Appl. Phys. Lett.*, 2011, **98**, 164101.
133. A. Khaldi, C. Plesse, C. Soyer, C. Chevrot, D. Teyssié, F. Vidal and E. Cattan, *Proc. SPIE - Smart Mater. Struct.*, 2012, **8340**, 83400J–1-83400J–9.
134. A. Khaldi, C. Plesse, C. Soyer, E. Cattan, F. Vidal, C. Chevrot and D. Teyssié, *Proc. ASME 2011 Int. Mech. Eng. Congr. Expo.*, 2011, **1**, 1–3.
135. A. Maziz, C. Plesse, C. Soyer, C. Chevrot, D. Teyssié, E. Cattan and F. Vidal, *Adv. Funct. Mater.*, 2014, **24**, 4851–4859.
136. A. Maziz, C. Plesse, C. Soyer, E. Cattan and F. Vidal, *Proc. SPIE*, 2015, **9430**, 1–8.
137. A. Khaldi, D. Falk, K. Bengtsson, A. Maziz, D. Filippini, N. D. Robinson and E. W. H. Jager, *ACS Appl. Mater. Interfaces*, 2018, **10**, 14978–14985.
138. A. Khaldi, A. Maziz, G. Alici, G. M. Spinks and E. W. H. Jager, *SPIE Smart Struct. Mater. Nondestruct. Eval. Heal. Monit.*, 2015, **9430**, 94301R.
139. A. Khaldi, A. Maziz, G. Alici, G. M. Spinks and E. W. H. Jager, *Sens. Actuators, B*, 2016, **230**, 818–824.
140. A. Maziz, C. Plesse, C. Soyer, E. Cattan and F. Vidal, *ACS Appl. Mater. Interfaces*, 2016, **8**, 1559–1564.
141. Y. Zhong, S. Lundemo and E. W. H. Jager, *Smat Mater. Struct.*, 2018, **27**, 1–7.
142. K. Rohtlaid, G. T. M. Nguyen, C. Soyer, E. Cattan, F. Vidal and C. Plesse, *Adv. Electron. Mater.*, 2019, **5**, 1–11.
143. K. Rohtlaid, *PhD thesis Univ. Paris-Seine*, 2019.